

Electronic Supplementary Information

Naphthalene anhydride triphenylamine as a viscosity-sensitive molecular rotor for liquid safety inspection

Lingfeng Xu ^{a,b,*}, Xinkang Peng ^a, Gengxiang Ma ^c, Mei Zeng ^a, Kui Wu ^a, Limin Liu ^{a,*}

^a School of Chemistry and Chemical Engineering, Jinggangshan University, Ji'an, Jiangxi 343009, China

^b State Key Laboratory of Luminescent Materials & Devices, Guangdong Provincial Key Laboratory of Luminescence from Molecular Aggregates, College of Materials Science & Engineering, South China University of Technology, Guangzhou 510640, China

^c School of Chemistry and Chemical Engineering, Dezhou University, Dezhou, Shandong 253026, China.

* Corresponding author. E-mail: rs7lfxu@outlook.com

E-mail: llm24@126.com

Table of contents

Experimental section.....	S1
Scheme S1.....	S7
Fig. S1.....	S8
Fig. S2.....	S9
Fig. S3.....	S10
Fig. S4.....	S11
Fig. S5.....	S12
Fig. S6.....	S13
Fig. S7.....	S13
Fig. S8.....	S14
Fig. S9.....	S15
Fig. S10.....	S15
Fig. S11.....	S16
Fig. S12.....	S16
Fig. S13.....	S17
Fig. S14.....	S18
Fig. S15.....	S19
Fig. S16.....	S20
Fig. S17.....	S21
Fig. S18.....	S22
Table S1.....	S23
Table S2.....	S25
Table S3.....	S25
References.....	S26

Experimental section

Materials and methods

4-Bromo-1,8-naphthalic anhydride, propylamine, 4-bromo-N,N-diphenylaniline, 4,4,4',4',5,5,5',5'-octamethyl-2,2'-bi(1,3,2-dioxaborolane), palladium acetate ($\text{Pd}(\text{OAc})_2$), tetrabutylammonium bromide (TBAB), potassium carbonate, tetrahydrofuran (THF), toluene, dichloromethane (DCM), dimethylsulfoxide (DMSO), N,N-dimethylformamide (DMF), methanol, ethanol, ethyl acetate, acetonitrile, phosphate buffer solution (PBS) and various metal salts such as the sodium chloride, calcium chloride, magnesium sulphate, and so on, were purchased from Shanghai Aladdin Bio-Chem Technology Co., Ltd. Common food additives including the glucose, taurine, sodium carboxymethyl cellulose, arabic gum, xanthan gum were obtained from Bide pharmacy technology (Shanghai) Co., Ltd. The amino acids such as cysteine (Cys), homocysteine (Hcy), glutathione (GSH), nystatin and monensin were obtained from Sigma-Aldrich (Merck Life Sciences Co., Ltd., Shanghai, China). Dullbecco's Modified Eagle Medium (DMEM) and Roswell Park Memorial Institute (RPMI) 1640 complete medium, MTT (3-(4,5-dimethylthiazol-2-yl)-2,5-diphenyltetrazolium bromide) and trypsin-ethylenediaminetetraacetic acid disodium salt (EDTA) were purchased from Life Technologies, Thermo Fisher Scientific Co., Ltd, Shanghai, China. HeLa (human cervical cancer cells) and HepG2 (human liver carcinoma cells) were purchased from KeyGen Biology Co., Ltd, Nanjing, China. All the chemical reagents used in this work were of analytical grade and used as received. Triple distilled water was used in the experiments.

Nuclear magnetic resonance (NMR) spectra were acquired with a Bruker AVANCE III HD 600 NMR Spectrometer. High resolution mass spectra were obtained with an Agilent 7250 & JEOL-JMS-T100LP AccuTOF mass spectrometer. Fluorescence spectra were measured by a Hitachi F-7000 fluorescence spectrophotometer. Absorption spectra were recorded on a Hitachi U-3010 UV-vis spectrophotometer. The viscosity determination test was performed on a rotating viscometer (DV2T, Brookfield, AMETEK Corp., USA).

Synthesis procedure

Synthesis of 6-bromo-2-propyl-1H-benzo[de]isoquinoline-1,3(2H)-dione (Compound 1)

4-Bromo-1,8-naphthalic anhydride (277.1 mg, 1.0 mmol) was dissolved in ethanol, and the solution of propylamine (70.9 mg, 1.2 mmol) was added as well. The mixture was stirred under ambient temperature for half an hour under N₂ atmosphere, and potassium carbonate solution (2M) was injected dropwise in the upon mixture. Afterwards, the reaction system was performed at 68 °C, and refluxed overnight, and the reaction was monitored by TLC. After cooling down to room temperature, the solvent was removed in vacuum, the crude product obtained was purified through the silica-gel column chromatography using DCM/petroleum ether (v/v=1/1), the Compound 1 as a light yellow powder was obtained (251.33 mg, 79%). ¹H NMR (600 MHz, CDCl₃) δ 8.60 (dd, J = 7.2, 4.4 Hz, 2H), 8.48 (dd, J = 15.5, 8.9 Hz, 2H), 8.10 (d, J = 8.4 Hz, 1H), 3.41 (t, J = 7.2 Hz, 2H), 1.86 (dt, J = 13.9, 7.0 Hz, 2H), 1.14 (t, J = 7.4 Hz, 3H). MS (ESI): m/z 318.14142 [M]⁺.

Synthesis of 6-(4-(diphenylamino)phenyl)-2-propyl-1H-benzo[de]isoquinoline-1,3(2H)-dione (DPPBQD)

Compound 1 (318.1 mg, 1.0 mmol) and the 4-bromo-N,N-diphenylaniline (324.2 mg, 1.0 mmol) was dissolved in the toluene in the Schlenk flask. The potassium carbonate aqueous solution (2 M) and TBAB (161.2 mg, 0.5 mmol) was dropped into the above solution as well, followed with continuous stirring at ambient temperature under N₂ atmosphere for half an hour. Then the solution of 4,4,4',4',5,5,5',5'-octamethyl-2,2'-bi(1,3,2-dioxaborolane) (253.9 mg, 1.0 mmol) and palladium acetate (4.5 mg, 0.02 mmol) in THF was added dropwise to upon mixture, separately. Afterwards, the reaction system was refluxed overnight, and the reaction was monitored by Thin Layer Chromatography (TLC). Then, the solvent was removed under reduced pressure. The crude product was extracted with DCM, the organic phase was collected and dried over MgSO₄. Finally, the crude product was purified by the silica-gel column chromatography using DCM/petroleum ether (v/v=2/1) to afford the molecular rotor DPPBQD as an orange powder (395.41 mg, 82%). ¹H NMR (600 MHz, CD₃CN) δ 8.59 (d, J = 9.5 Hz, 1H), 8.45 (dd, J = 6.9, 5.6 Hz, 2H), 7.85-7.75 (m, 2H), 7.62 (d, J = 8.4 Hz, 2H), 7.48 (d, J = 8.5 Hz, 2H), 7.39 (t, J = 7.8 Hz, 4H), 7.26-7.09 (m, 6H), 4.16-4.07 (m, 2H), 1.76 (dt, J = 10.8, 5.8 Hz, 2H), 1.20-1.15 (m, 3H). MS (ESI): m/z 482.20804 [M]⁺.

Measurements of optical properties

The molecular rotor DPPBQD was dissolved in DMSO to prepare the stock solution with the concentration of 1 mM, and stored in the dark under the temperature of 3 °C.

During the test procedure, the concentration of DPPBQD was controlled as 10 μM . The viscosity determination procedure was as follows. The probe was added into a 3 mL solution consisting various volume percentages of distilled water and glycerol (from 0% to 99%, including 1% DMSO), and the fluorescence spectra and UV-Vis absorption measurements were operated in this mixture system. Corresponding viscosity values were recorded and measured by the viscometer. Solvents with various polarities, such as methanol, DMSO, DMF, etc. were selected to test the emission properties of molecular rotor DPPBQD in the complex solvent environment. DPPBQD was added into selected solvents and shook before the test. In the specificity test, the solutions with various potential interfering analytes (including NaCl, CaCl₂, glucose, and so on) were prepared with distilled water, and DPPBQD was added in each interfering test. The resulting solutions were mixed uniformly before the spectra were recorded. In the temperature effect experiment, DPPBQD was added into the glycerol under different temperature, such as the normal body temperature (37 °C), fresh-keeping temperature (5 °C) and common room temperature (25 °C) with 1% DMSO contained. In all measurements, the mixed solutions were transferred to the quartz cell. The excitation wavelength was set as 460 nm.

Theoretical calculations

The calculations were performed using the Gaussian09 program, ground state structure of the rotor was optimized using time-dependent density functional theory (TD-DFT) by using the B3LYP/6-31G(d) level of theory.

Fluorescence analysis of the thickening effect

Three kinds of food thickeners, such as sodium carboxymethyl cellulose, arabic gum, and xanthan gum with various mass concentrations (from 1 g/kg to 7 g/kg) were dissolved in the twice-distilled water, followed by the addition of DPPBQD dilution (10 μ M). Before the test, the mixtures were treated by ultrasound for 10 min to eliminate bubbles in the high-viscous solution, and placed under room temperature for 1 h.

Cytotoxicity determination

HeLa cells were cultured in Dullbecco's Modified Eagle Medium (DMEM), containing 10% FBS (Fetal Bovine Serum) and 1% penicillin & streptomycin at 37 °C in a humidified incubator containing 5% CO₂ and HepG2 cells were incubated in complete medium composed of 89% Roswell Park Memorial Institute (RPMI) 1640 with 10% fetal bovine serum (FBS) and 1% penicillin & streptomycin at 37 °C in a humidified incubator containing 5% CO₂, toxicities of molecular rotor DPPBQD toward HeLa cells and HepG2 cells were determined by using the MTT cell Proliferation and Cytotoxicity Assay Kit.

Cell imaging

The exponentially growing cells were seeded in six-well plates at 4×10^5 cells per dish and grown for 24 h. Then the cells were washed with PBS, and as for HeLa cells, some cells were incubated with complete medium with the molecular rotor DPPBQD (10 μ M) for 30 min, and some cells were incubated in complete medium with the monensin or the nystatin added for 30 min, and then were incubated with the rotor DPPBQD for another 30 min. Afterward, the cells were washed with PBS buffer three times and

fluorescence imaging was acquired using an Olympus IX71 inverted fluorescence microscope equipped with a DP72 color CCD.

Viscosity tracking in the food spoilage process

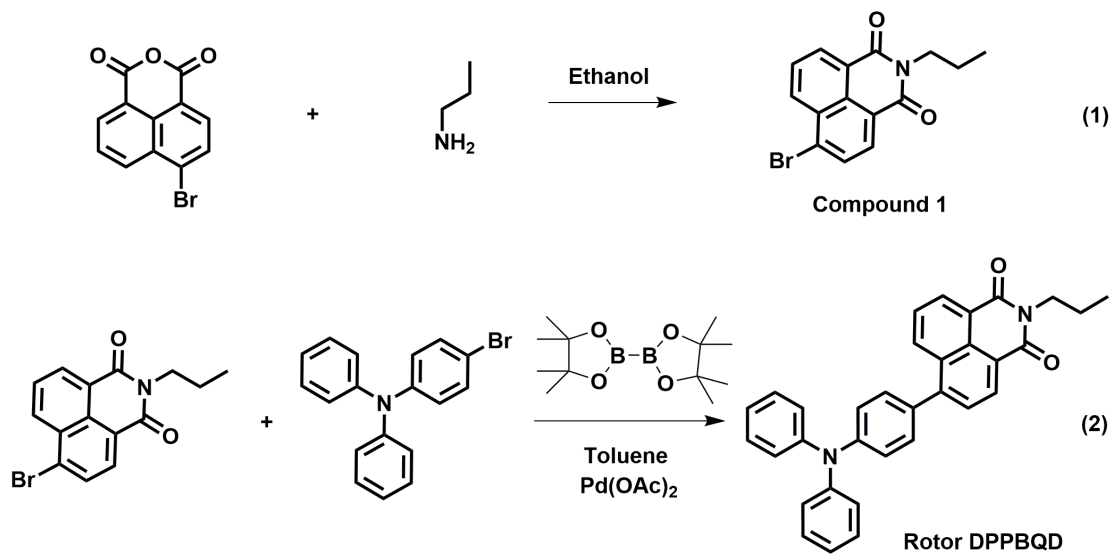
Two kinds of commercial liquid beverages, including the soup and coconut juice were stored at different temperature (25 °C & 5 °C) when exposed to the air for 8 days. The fluorescence emission spectra were recorded within this time interval (at day 0, day 3, day 5, day 8) with the addition of DPPBQD dilution (10 μM). The relationship between the fluorescence intensity enhancement and viscosity variation was fitted into the linear equation: $(\eta_n - \eta_0)/\eta_0 \sim (F_n - F_0)/F_0$, in which η_n and η_0 were defined as the viscosity of beverages at day 0 and day n ($0 < n < 9$), F_0 and F_n were displayed as the fluorescence intensity of beverages at day 0 and day n ($0 < n < 9$).

The Förster–Hoffmann equation

According to the previous studies,^{1,2} the relationship between the fluorescence intensity of the molecular rotor DPPBQD and the viscosity can be determined through the following Förster-Hoffmann equation:

$$\log I = C + x \log \eta \quad (1)$$

where η represents the viscosity, I represents the fluorescence intensity of the molecular rotor DPPBQD at 590 nm, C is a constant, and x represents the sensitivity of the molecular rotor towards viscosity.



Scheme S1. Synthetic route and reaction conditions for the molecular rotor DPPBQD.

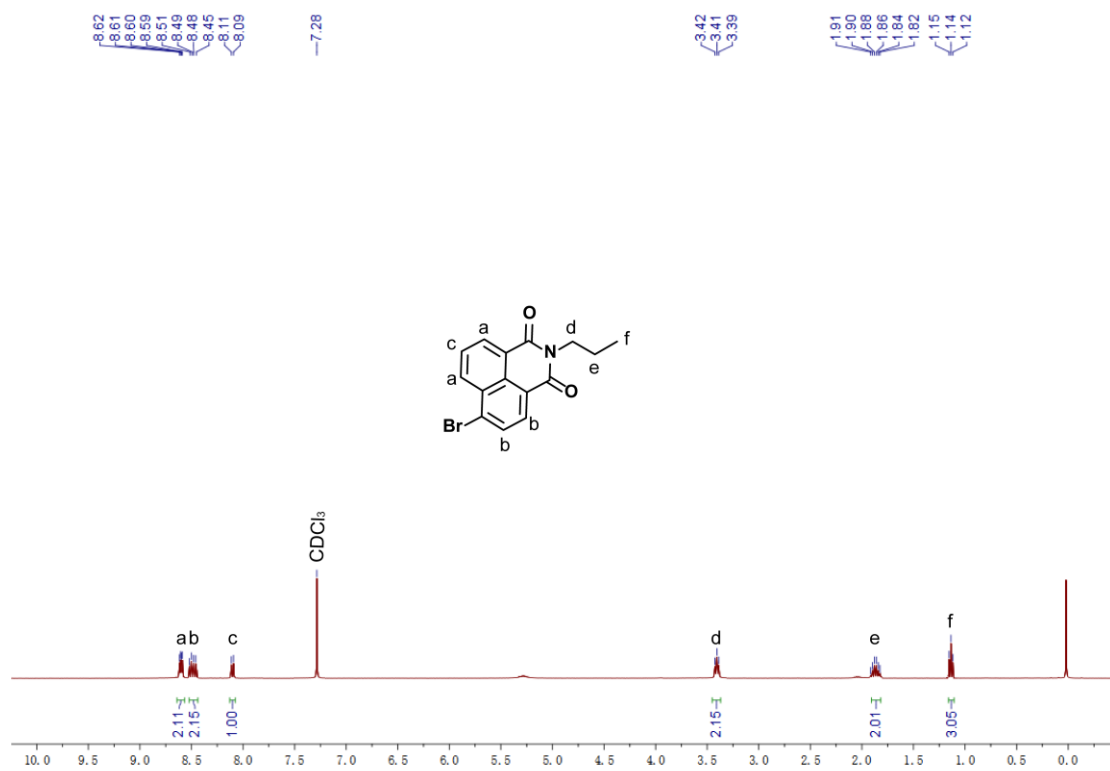


Fig. S1 ¹H-NMR spectrum of Compound 1 in CDCl₃.

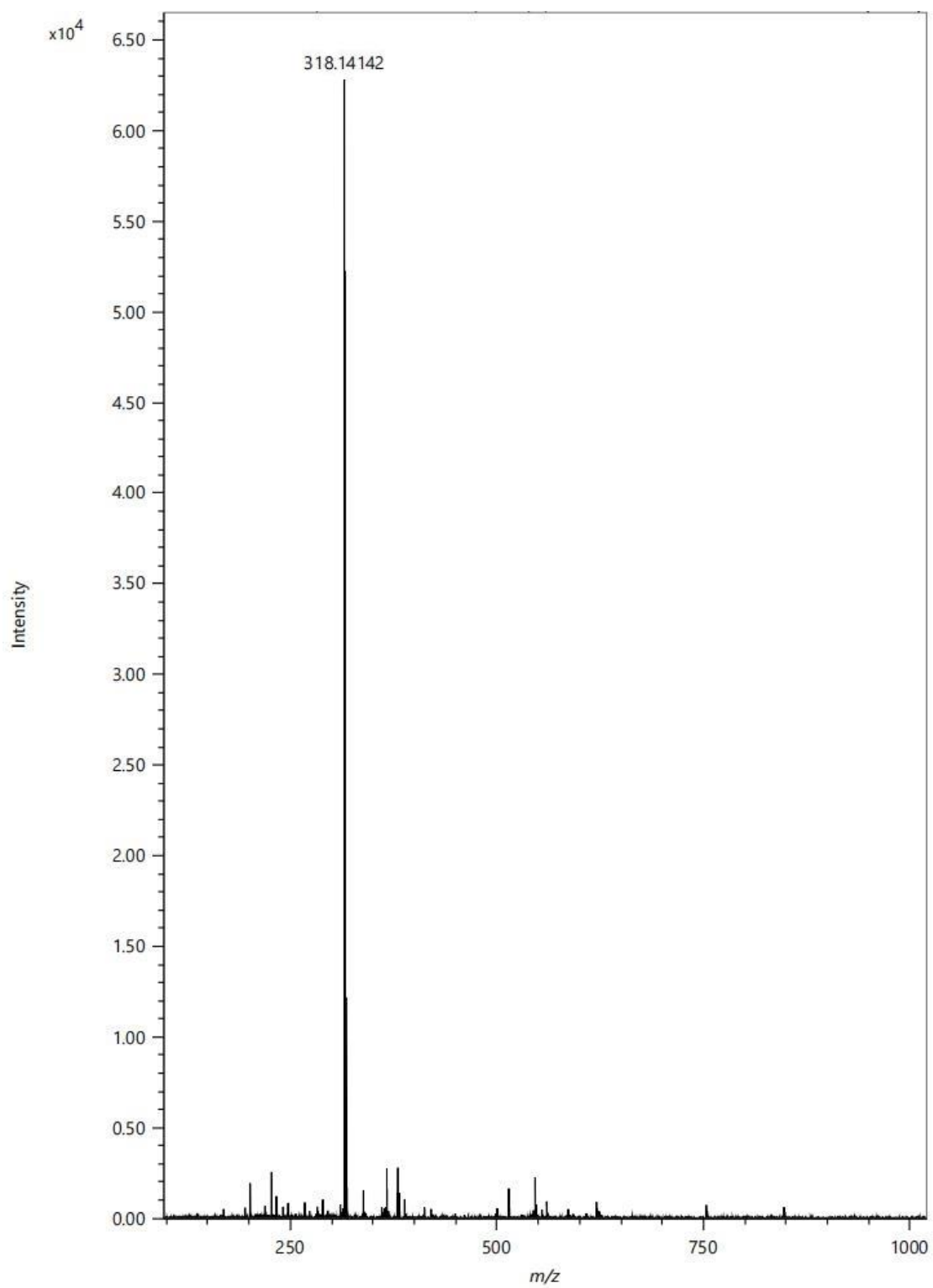


Fig. S2 HR mass spectrum of Compound 1. MS (ESI): m/z 318.14142 $[M]^+$.

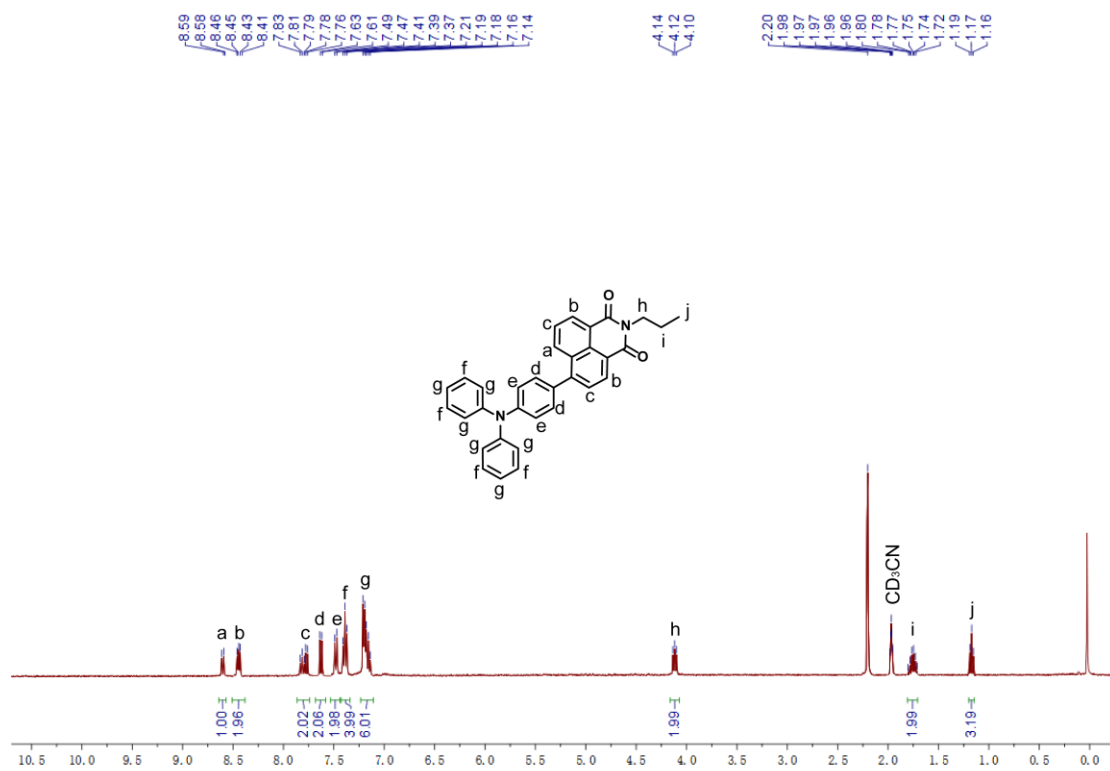


Fig. S3 ¹H-NMR spectrum of the molecular rotor DPPBQD in CD₃CN.

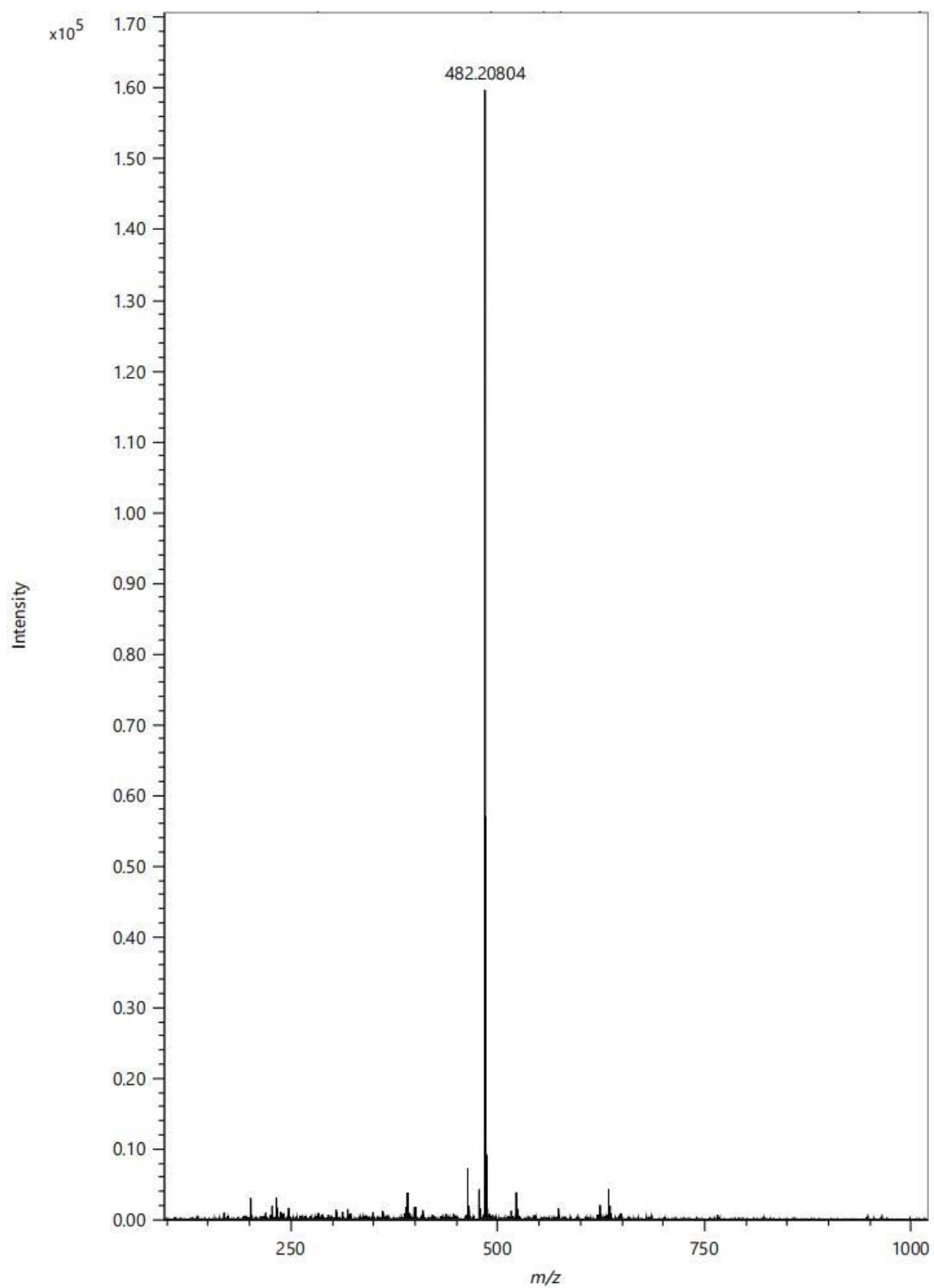


Fig. S4 HR mass spectrum of the molecular rotor DPPBQD. MS (ESI): m/z 482.20804
[M]⁺.

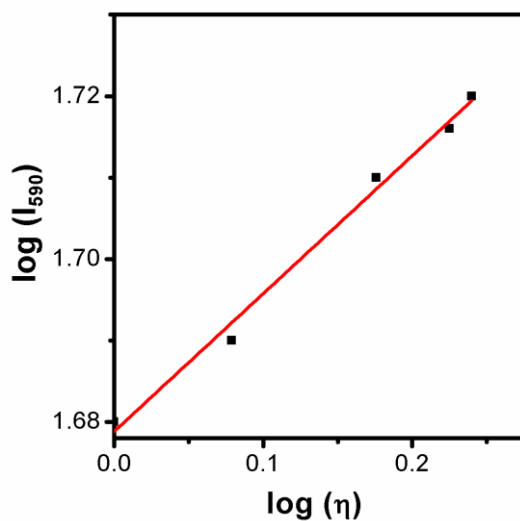


Fig. S5 Log (I_{590}) as a function of log (η).

Determination of the detection limit:

The calibration curve was first obtained from the plot of log (I_{590}) as a function of log (η). Then the regression curve equation was obtained for the lower viscosity part.

The detection limit = $3 \times S.D./k$

Where k is the slope of the curve equation, and $S.D.$ represents the standard deviation for the log (I_{590}) of molecular rotor DPPBQD.

$$\log(I_{590}) = 1.678 + 0.169 \times \log(\eta) \quad (R^2 = 0.991)$$

$$\log(\text{LOD}) = 3 \times 0.002/0.169 = 0.036$$

$$\text{LOD} = 10^{0.036} = 1.086 \text{ cP}$$

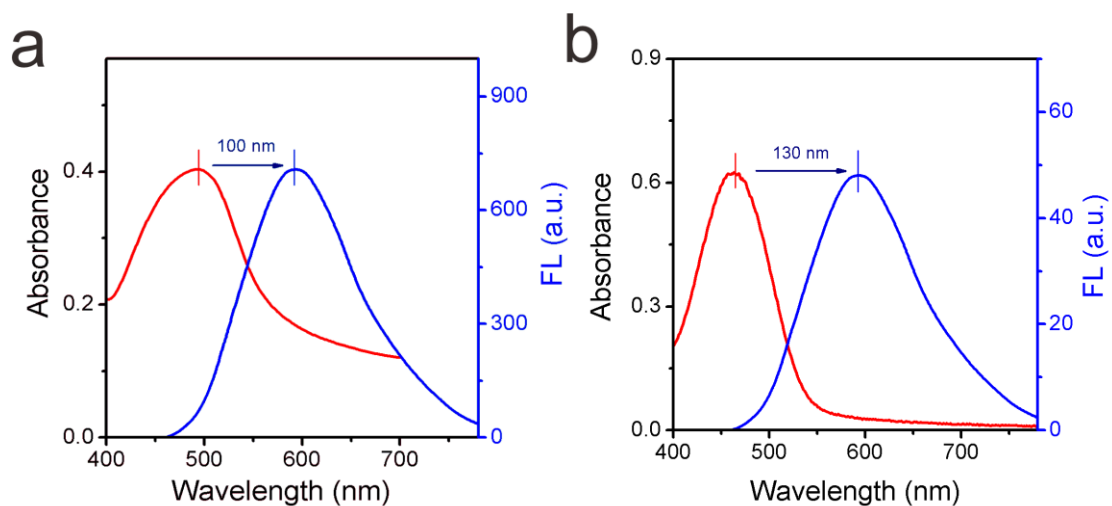


Fig. S6 (a) Fluorescence spectrum (blue curve) and absorption spectrum (red curve) of the molecular rotor DPPBQD in glycerol (containing 1% DMSO). (b) Fluorescence spectrum (blue curve) and absorption spectrum (red curve) of the molecular rotor DPPBQD in water (containing 1% DMSO).

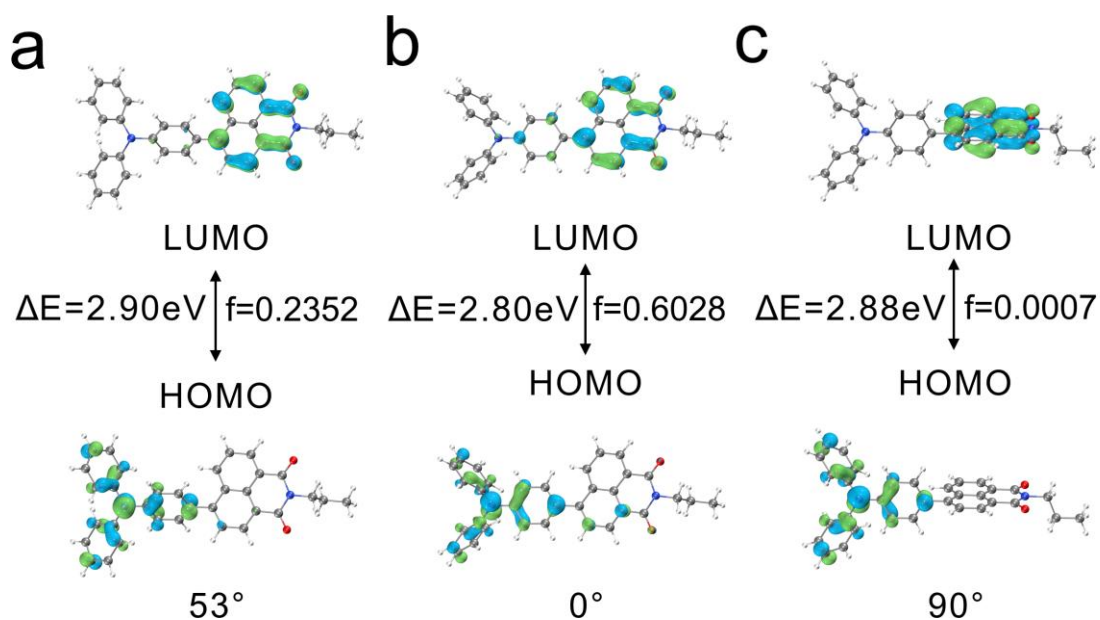


Fig. S7 Optimized molecular structures and calculated molecular orbital energy levels of the HOMO and LUMO of DPPBQD based on B3LYP/6-31G basis set.

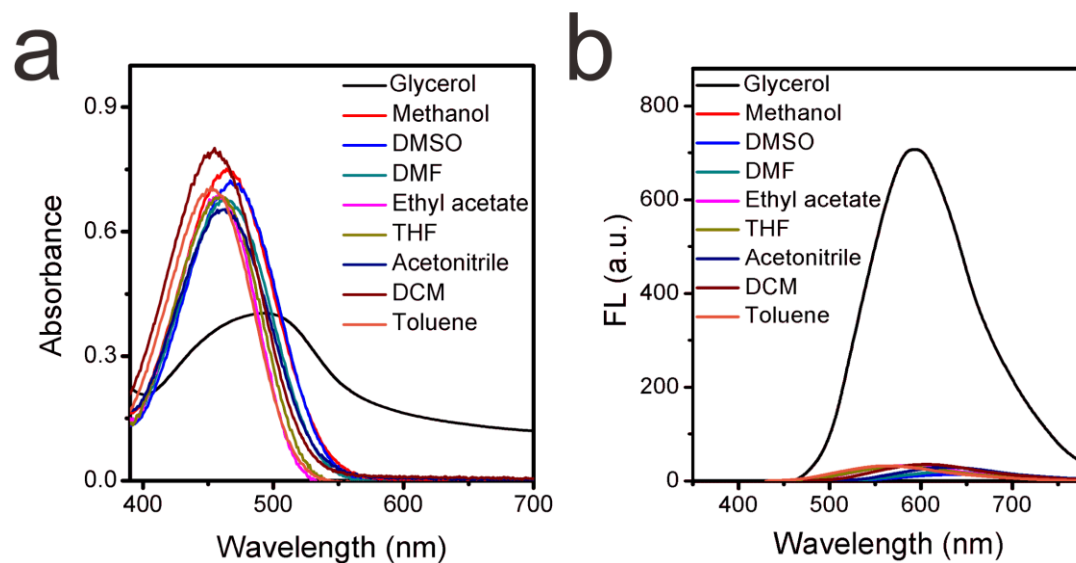


Fig. S8 (a) The absorption spectra of the molecular rotor DPPBQD (10 μM) in various common solvents. (b) The fluorescent spectra of the molecular rotor DPPBQD (10 μM) in various common solvents. $\lambda_{\text{ex}}=460$ nm.

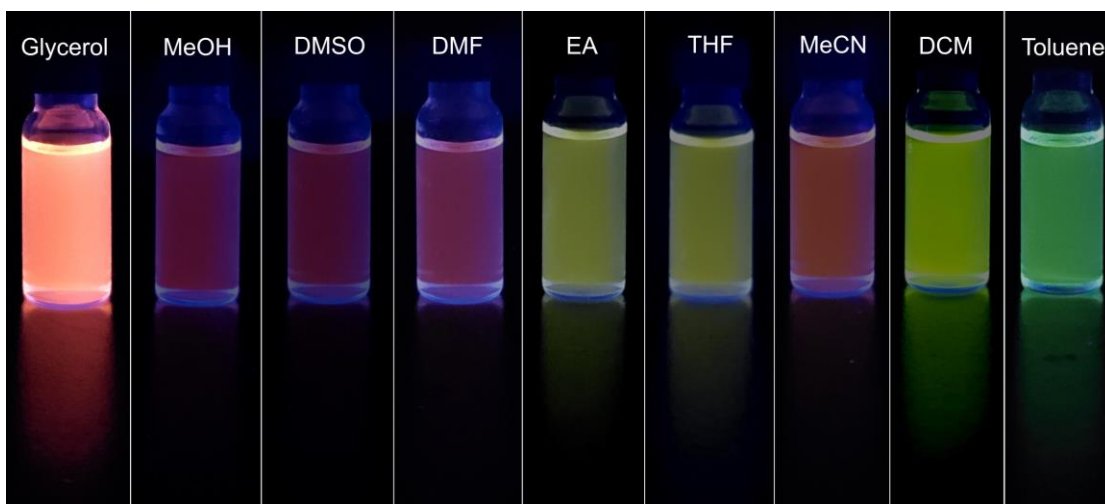


Fig. S9 Fluorescence image of the rotor DPPBQD in various solvents.

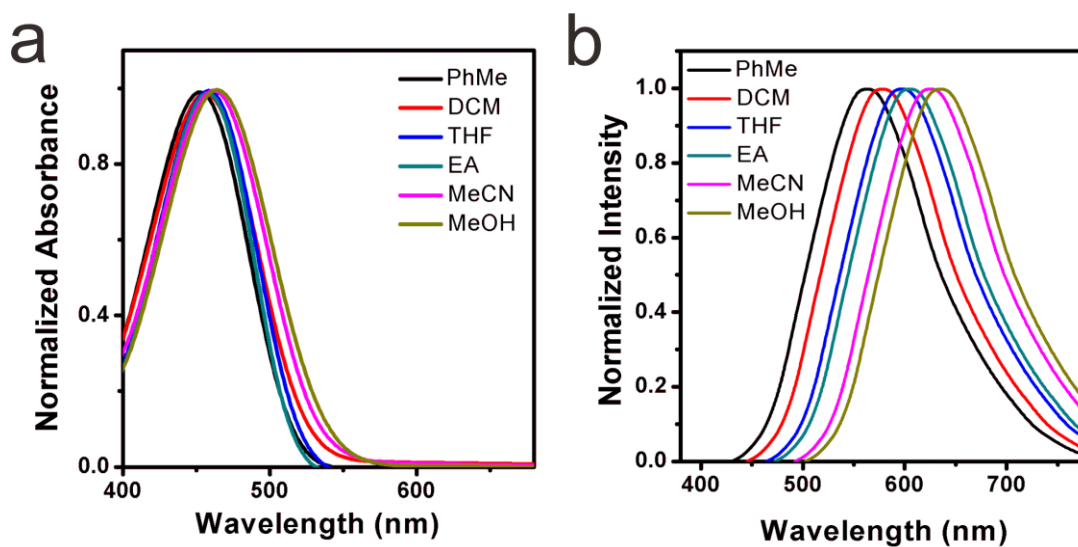


Fig. S10 (a) Normalized absorption spectra of molecular rotor DPPBQD in six kinds of common solvents; (b) Normalized fluorescence emission spectra in six kinds of common solvents.

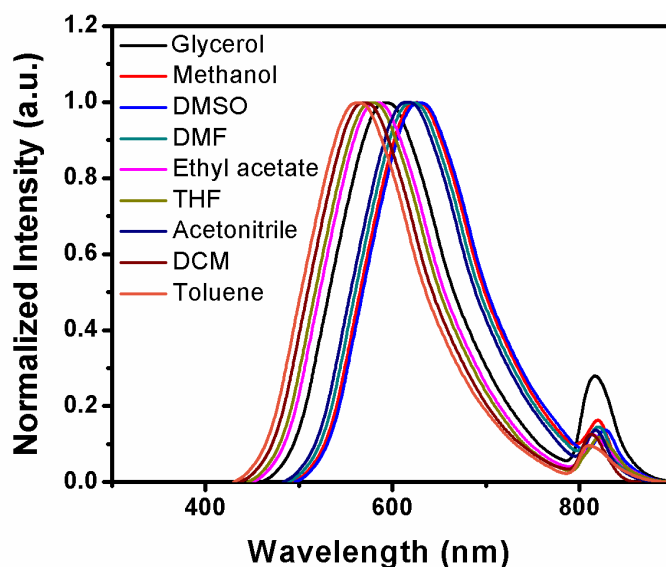


Fig. S11 Normalized dual emission spectra of the rotor DPPBQD in various solvents.

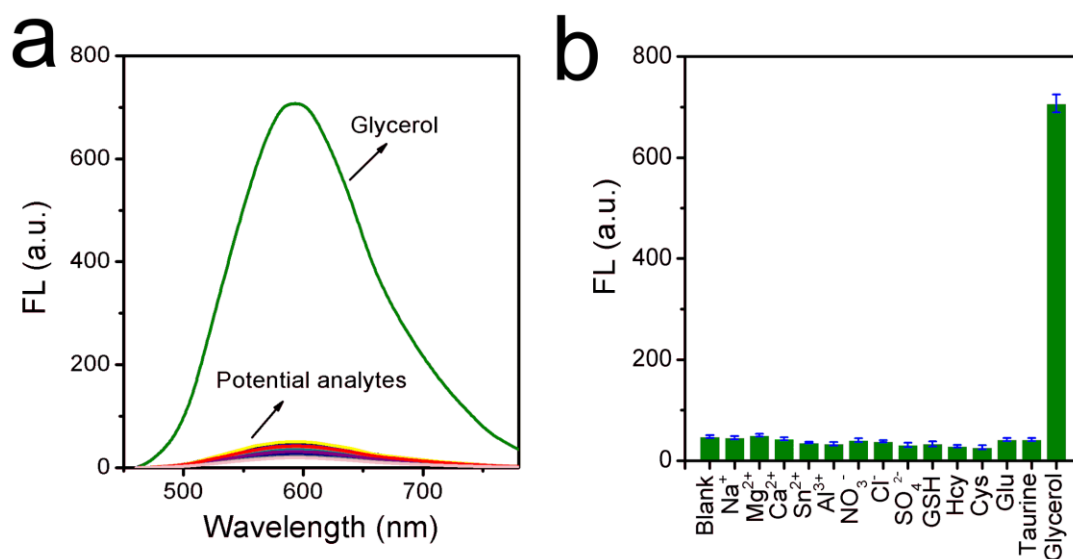


Fig. S12 (c) Fluorescence spectra of the rotor DPPBQD (10 μM) in the glycerol and in the absence or presence of other potential analytes (100 μM) in water respectively, including the Na^+ , Mg^{2+} , Ca^{2+} , Sn^{2+} , Al^{3+} , NO_3^- , Cl^- , SO_4^{2-} , GSH, Hcy, Cys, glucose (Glu), taurine. (d) Fluorescence intensity of the rotor DPPBQD (10 μM) at 590 nm in the glycerol and with the existence of various potential analytes (100 μM) in water, respectively.

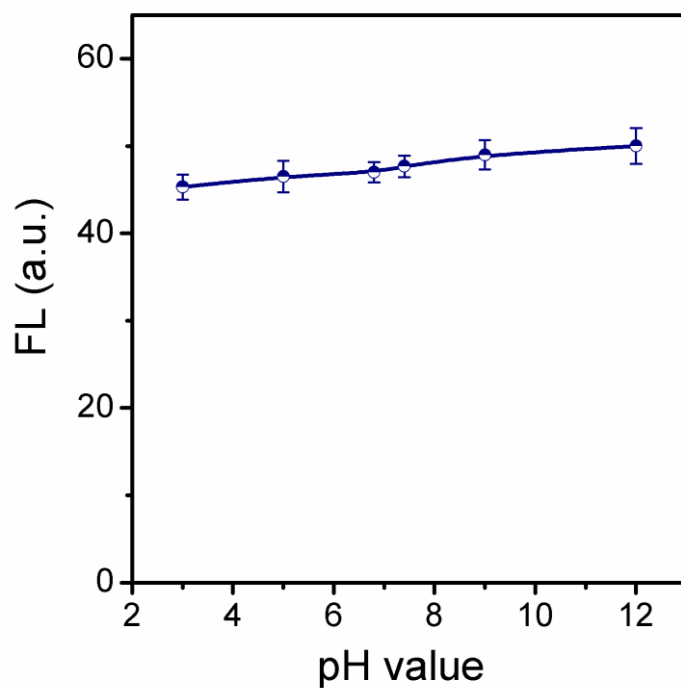


Fig. S13 Fluorescence intensity of the molecular rotor DPPBQD at 590 nm with various pH values (in disodium hydrogen phosphate-citric acid and disodium hydrogen phosphate-sodium hydrogen acid buffer solutions), $\lambda_{\text{ex}}=460$ nm.

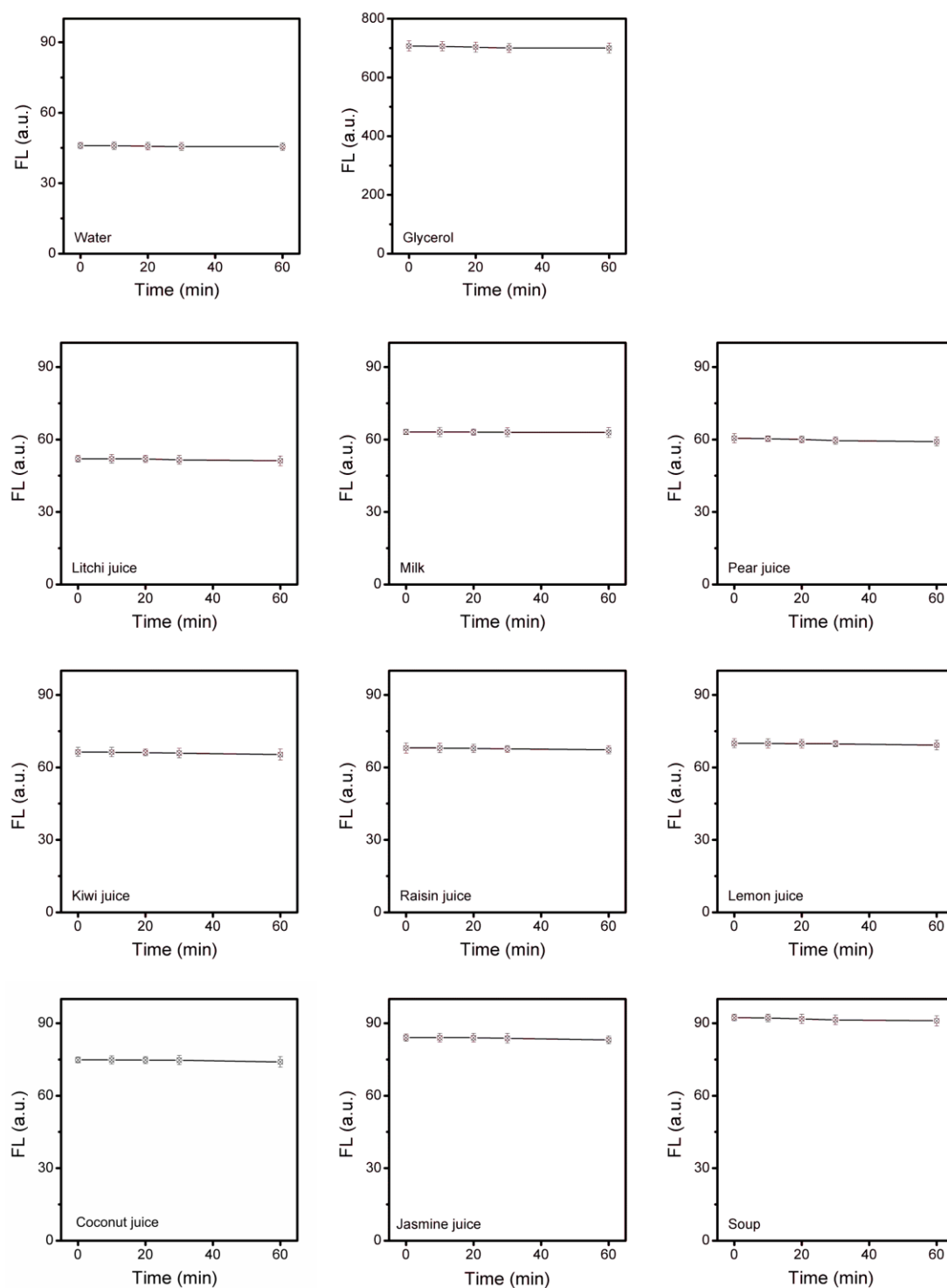


Fig. S14 Photostability analysis of the molecular rotor DPPBQD in the water, the glycerol and nine kinds of common liquid food (containing 1% DMSO). All the samples were tested under continuous light irradiation with UV lamp.

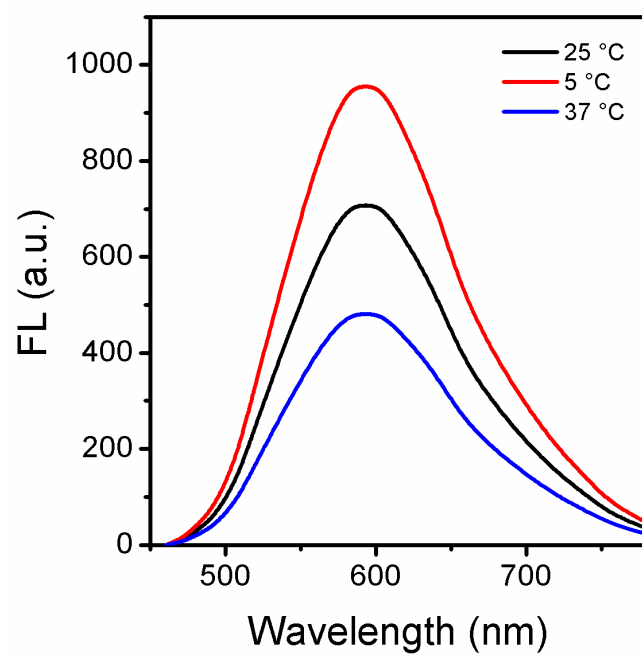


Fig. S15 Fluorescence spectra of the molecular rotor DPPBQD (10 μM) in glycerol under the ambient temperature (25 °C), fresh-keeping temperature (~5 °C) and normal body temperature (37 °C).

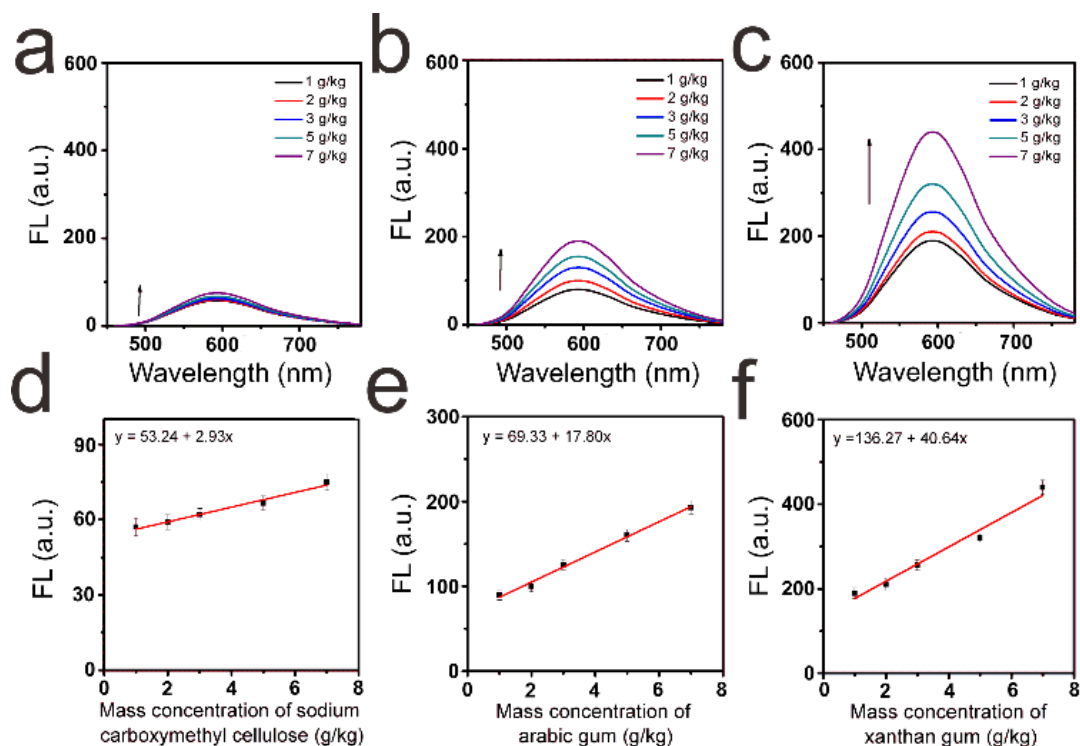


Fig. 16 (a) Fluorescence spectra of the molecular rotor DPPBQD (10 μM) with the existence of different mass contents of sodium carboxymethyl cellulose in water. (b) Fluorescence spectra of the molecular rotor DPPBQD (10 μM) with the existence of different mass contents of arabic gum in water. (c) Fluorescence spectra of the molecular rotor DPPBQD (10 μM) with the existence of different mass contents of xanthan gum in water. (d) Fitting linear relationship of fluorescence intensities of the rotor DPPBQD (10 μM) at 590 nm with various mass contents of sodium carboxymethyl cellulose addition. (e) Fitting linear relationship of fluorescence intensities of the rotor DPPBQD (10 μM) at 590 nm with various mass contents of arabic gum addition. (f) Fitting linear relationship of fluorescence intensities of the rotor DPPBQD (10 μM) at 590 nm with various mass contents of xanthan gum addition.

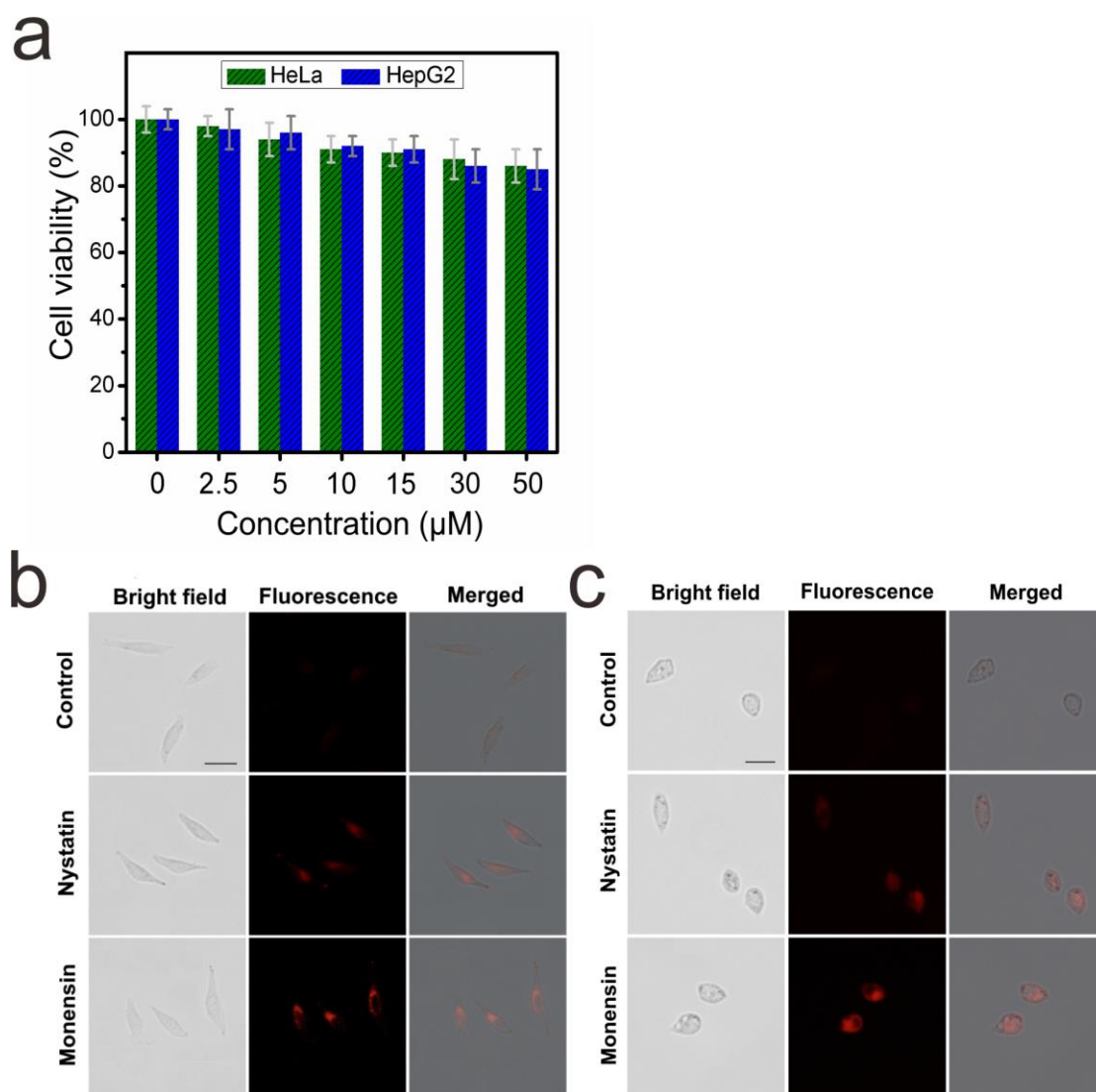


Fig. S17 (a) Cytotoxic effects against HeLa and HepG2 cells upon 24 hours of incubation with different concentrations of the molecular rotor DPPBQD; (b) Fluorescence microscopy images of HeLa cells incubated with 10 μM free rotor DPPBQD for 30 min, or with pretreatment of nystatin, monensin for 30 min; (c) Fluorescence microscopy images of HepG2 cells incubated with 10 μM free rotor DPPBQD for 30 min, or with pretreatment of nystatin, monensin for 30 min. Scale bar: 20 μm

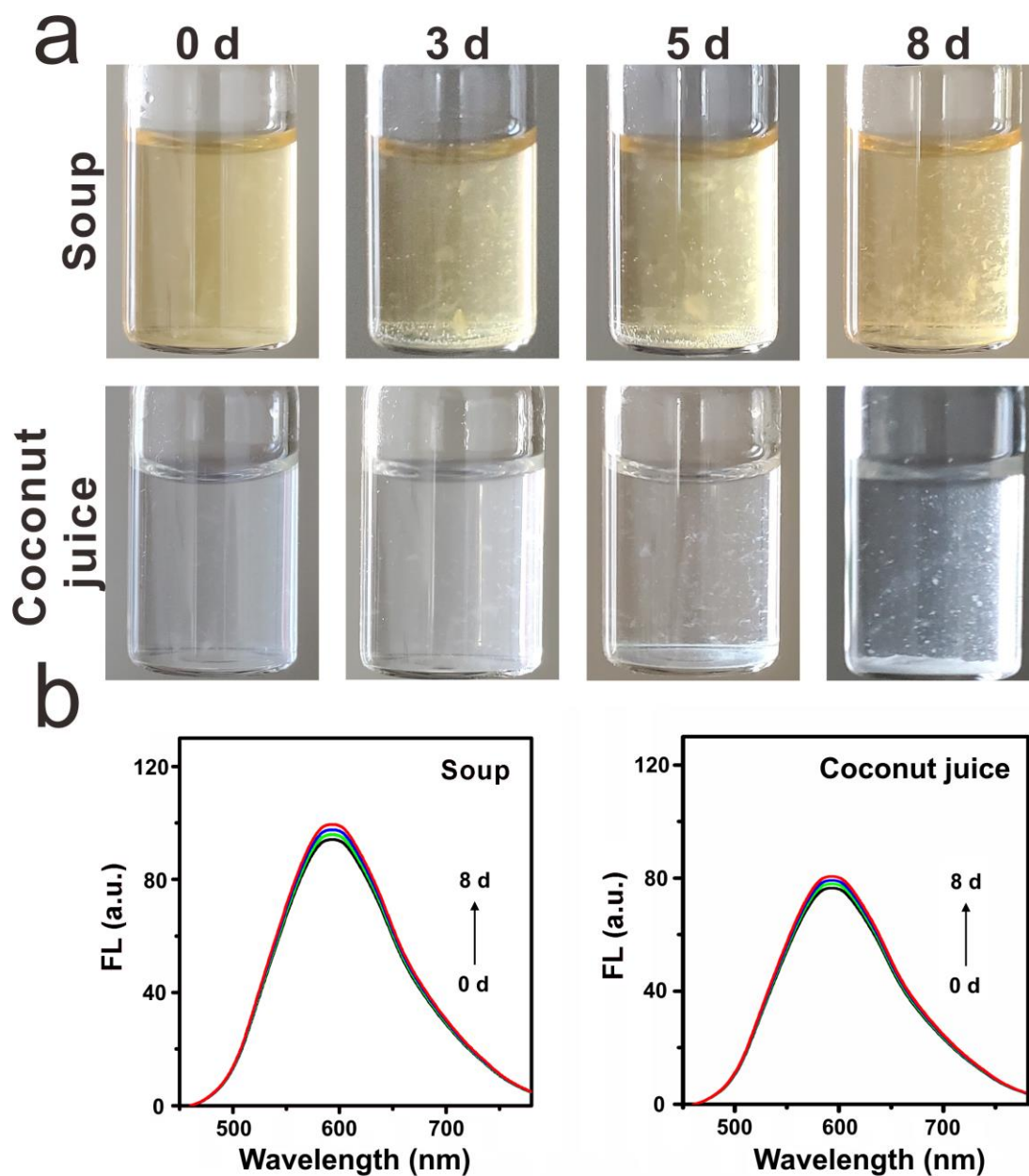
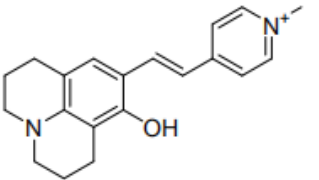
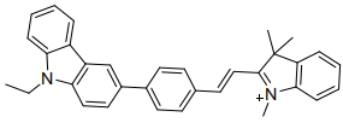
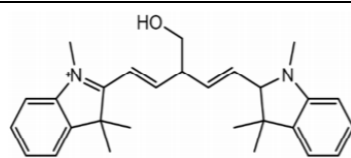
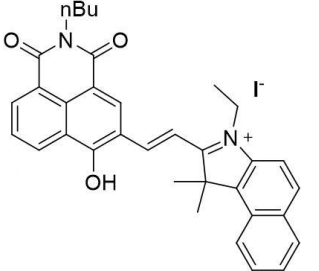
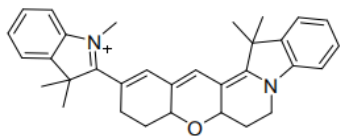
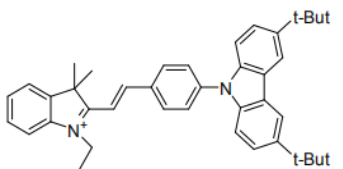
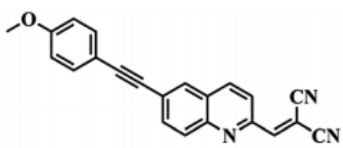
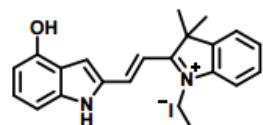
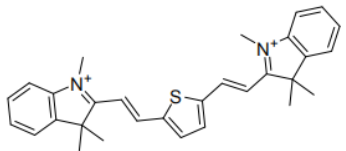
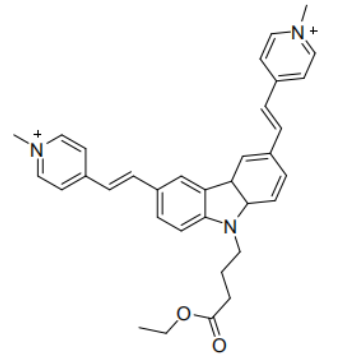
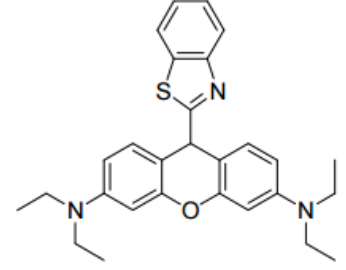
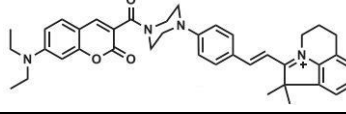
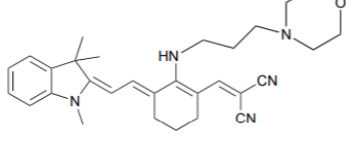
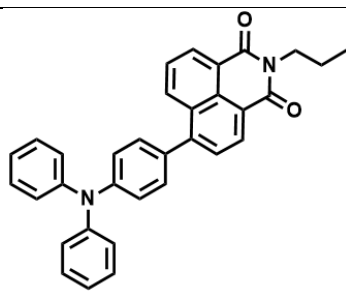


Fig. S18 (a) Digital images of the soup and coconut juice that stored under fresh-keeping temperature (~ 5 °C) for varying time (from day 0 to day 8). (b) Fluorescent spectra of the soup and coconut juice stored under fresh-keeping temperature (~ 5 °C) at different time intervals.

Table S1. Comparison of the representative fluorescence-based dyes for viscosity detection reported in recent years.

Probe	λ_{ab}^*	λ_{em}^{**}	Stokes shift (nm)	Application	Reference
	530 nm	620 nm	90 nm	Biological system, living cells.	3
	520 nm	610 nm	90 nm	Biological system, living cells, in vitro, zebrafish.	4
	550 nm	571 nm	21 nm	Biological system, living cells.	5
	580 nm	635 nm	55 nm	Biological system, living cells.	6
	678 nm	698 nm	20 nm	Biological system, living cells, rat slice.	7
	545 nm	628 nm	83 nm	Biological system, living cells.	8
	400 nm	470 nm	70 nm	Biological system, living cells.	9
	510 nm	600 nm	90 nm	Biological system, living cells, ex vivo.	10

	525 nm	595 nm	70 nm	Biological system, living cell.	11
	470 nm	560 nm	90 nm	Biological system, living cell.	12
	600 nm	635 nm	35 nm	Biological system, living cells.	13
	520 nm	580 nm	60 nm	Biological system, living cell.	14
	565 nm	620 nm	55 nm	Biological system, living cell.	15
	490 nm	590 nm	100 nm	Liquid food, food safety analysis.	This work

* Absorption peak. The absorption was measured in the glycerol.

** Emission peak. The fluorescence emission was measured in the glycerol.

*** The Stokes shift herein was obtained from the absorption and emission spectra measured in the glycerol.

Table S2. Optical properties of the molecular rotor DPPBQD.

Emitter	λ_{em} (nm)	
DPPBQD	Quantum yield in ethanol (Φ)*	Quantum yield in glycerol (Φ)*
	0.7%	14.3%

* Estimated using Rhodamine B as the standard ($\Phi_F = 50\%$ in ethanol).

Table S3. Photo-physical properties of the molecular rotor DPPBQD in different solvents with different polarities.

Solvents	Dielectric constant (ϵ)	η^* (cP)	Absorption λ_{ab} (nm)	Emission λ_{em} (nm)
Glycerol	45.8	956.0	490.0	590.0
Methanol	32.6	0.6	464.5	623.7
DMSO	46.8	2.1	469.6	626.0
DMF	36.7	0.8	463.8	622.0
Ethyl acetate	6.1	0.45	458.3	580.9
THF	7.4	0.5	457.8	578.5
Acetonitrile	37.5	0.4	461.2	618.9
DCM	8.9	0.4	454.5	568.2
Toluene	2.4	0.6	452.5	560.8

* Viscosity of the solvent.

References

- 1 I. E. Steinmark, P.-H. Chung, R. M. Ziolk, B. Cornell, P. Smith, J. A. Levitt, C. Tregidgo, C. Molteni, G. Yahioğlu, C. D. Lorenz and K. Suhling, *Small*, 2020, **16**, 1907139.
- 2 Y. Zhang, Q. Zhou, Y. Bu, T. Xu, X. Zhu, J. Zhang, Z. Yu, L. Wang, F. Zhong and H. Zhou, *Anal. Chim. Acta*, 2021, 338847.
- 3 B. Chen, C. Li, J. Zhang, J. Kan, T. Jiang, J. Zhou and H. Ma, *Chem. Commun.*, 2019, **55**, 7410–7413.
- 4 J. Yin, M. Peng and W. Lin, *Anal. Chem.*, 2019, **91**, 8415–8421.
- 5 Y. Wu, W. Shu, C. Zeng, B. Guo, J. Shi, J. Jing and X. Zhang, *Dye. Pigment.*, 2019, **168**, 134–139.
- 6 L.-L. Li, K. Li, M.-Y. Li, L. Shi, Y.-H. Liu, H. Zhang, S.-L. Pan, N. Wang, Q. Zhou and X.-Q. Yu, *Anal. Chem.*, 2018, **90**, 5873–5878.
- 7 S. J. Park, B. K. Shin, H. W. Lee, J. M. Song, J. T. Je and H. M. Kim, *Dye. Pigment.*, 2020, **174**, 108080.
- 8 K. Zhou, M. Ren, B. Deng and W. Lin, *New J. Chem.*, 2017, **41**, 11507–11511.
- 9 P. Ning, P. Dong, Q. Geng, L. Bai, Y. Ding, X. Tian, R. Shao, L. Li and X. Meng, *J. Mater. Chem. B*, 2017, **5**, 2743–2749.
- 10 W. Wang, Y. Liu, J. Niu and W. Lin, *Analyst*, 2019, **144**, 6247–6253.
- 11 Y. Baek, S. J. Park, X. Zhou, G. Kim, H. M. Kim and J. Yoon, *Biosens. Bioelectron.*, 2016, **86**, 885–891.
- 12 Z. Zou, Q. Yan, S. Ai, P. Qi, H. Yang, Y. Zhang, Z. Qing, L. Zhang, F. Feng and R. Yang, *Anal. Chem.*, 2019, **91**, 8574–8581.
- 13 M. Ren, L. Wang, X. Lv, J. Liu, H. Chen, J. Wang and W. Guo, *J. Mater. Chem. B*, 2019, **7**, 6181–6186.
- 14 L. He, Y. Yang and W. Lin, *Anal. Chem.*, 2019, **91**, 15220–15228.
- 15 H. Tan, Y. Qiu, H. Sun, J. Yan and L. Zhang, *Chem. Commun.*, 2019, **55**, 2688–2691.